Journal of
Composites Science

MDPI

Article

Effects of Polyphosphoric Acid on Physical, Rheological, and Chemical Properties of Styrene-Butadiene-Styrene (SBS)-Modified Asphalt Binder

Amjad H. Albayati [1], Mazen J. Al-Kheetan [2,*], Aliaa F. Al-ani [1], Yu Wang [3], Ahmed M. Mohammed [1] and Mustafa M. Moudhafar [1]

[1] Department of Civil Engineering, University of Baghdad, Baghdad 17001, Iraq
[2] Department of Civil and Environmental Engineering, College of Engineering, Mutah University, Karak 61710, Jordan
[3] School of Science, Engineering & Environment, University of Salford, Manchester M5 4WT, UK
* Correspondence: mazen.al-kheetan@mutah.edu.jo

Abstract: High temperatures combined with heavy traffic load necessitate asphalt binder modification to enhance its performance and durability. This research examines the effects of polyphosphoric acid (PPA) on the physical, rheological, and chemical properties of styrene-butadiene-styrene (SBS)-modified asphalt binders. Asphalt binders were prepared by adding 3% SBS and varying PPA dosages of 0.3%, 0.6%, and 0.9% by weight of asphalt cement. The experiment investigated the physical properties (penetration, softening point, ductility, viscosity, and specific gravity), the rheological properties (the performance grading (PG), multi-stress creep recovery (MSCR), and linear amplitude sweep (LAS)), and the microstructure and chemical composition of the modified asphalt binder. The results demonstrated impressive improvements in rutting resistance and stiffness. Adding 3% SBS and 0.9% PPA increased the rutting factor (G*/sin δ) by 165% and the high-temperature PG from 74.2 °C to 93.6 °C compared to the virgin asphalt binder. However, the optimum fatigue resistance was obtained by adding 0.3% PPA to the SBS asphalt binder. The microstructure and composition analysis revealed that using SBS and PPA together enhanced binder homogeneity and reduced voids. Lastly, an Overall Desirability (OD) analysis suggested the 3% SBS and 0.3% PPA to be the most effectively balanced formulation for the demand of high temperature and heavy traffic conditions. However, further field studies are recommended to validate the results under real-world conditions.

Keywords: polyphosphoric acid (PPA); SBS-modified asphalt; rheological properties; MSCR; LAS

check for updates

Academic Editors: Tri Ho Minh Le and Sangyum Lee

Received: 9 January 2025
Revised: 5 February 2025
Accepted: 6 February 2025
Published: 9 February 2025

Citation: Albayati, A.H.; Al-Kheetan, M.J.; Al-ani, A.F.; Wang, Y.; Mohammed, A.M.; Moudhafar, M.M. Effects of Polyphosphoric Acid on Physical, Rheological, and Chemical Properties of Styrene-Butadiene-Styrene (SBS)-Modified Asphalt Binder. *J. Compos. Sci.* **2025**, *9*, 78. https://doi.org/10.3390/jcs9020078

Copyright: © 2025 by the authors. Licensee MDPI, Basel, Switzerland. This article is an open access article distributed under the terms and conditions of the Creative Commons Attribution (CC BY) license (https://creativecommons.org/licenses/by/4.0/).

1. Introduction

High temperature and heavy traffic load present significant challenges to the performance and durability of asphalt pavement infrastructures. These factors necessitate continuous advancements in asphalt modification techniques to enhance its physical and rheological properties, aiming to improve pavement resistance to rutting, cracking, and aging under severe service conditions [1–3]. Among various modifiers, styrene-butadiene-styrene (SBS) and polyphosphoric acid (PPA) have gained considerable attention due to their unique and complementary properties [4]. SBS-modified binders have demonstrated superior elasticity with a stable performance across a broader temperature range compared to virgin asphalt binders [5]. Gao et al. [6] highlighted the effectiveness of SBS in reducing

fatigue-induced cracking under repetitive loading. However, SBS-modified binders also still face challenges, such as increased stiffness with aging, which deteriorates the flexibility of pavements [7–9]. In this situation, introducing complementary modifiers like PPA into the SBS asphalt binder has attracted increasing interest. PPA, an inorganic acid, has emerged as a promising additive to improve asphalt binder properties, particularly under high-temperature conditions. Studies by Ramayya et al. [10] and Liang et al. [11] have shown that PPA enhances binders' stiffness, softening point, and resistance to permanent deformation by altering binders' chemical structure. Xiao et al. [12] reported that increasing PPA content in asphalt binders resulted in higher rutting resistance, improved viscosity, and greater elasticity. Moreover, PPA helps enhance the aging resistance of asphalt binders [6]. PPA is considered cost-effective, with only a very small amount of PPA needed to improve the effectiveness of the properties of binders. With costs estimated at half or even less than those of polymer modifiers, PPA has become a practical choice for large-scale applications, where it has been adopted by many countries worldwide, such as the United States, where 16% of the asphalt is modified with PPA [13–15].

The synergistic combination of SBS and PPA has been explored in recent studies to capitalize on their complementary effects. For example, Li et al. [16] found that combining 0.75% PPA with SBS improved the rutting resistance of asphalt binders by 120% compared to SBS-modified binders alone. Wei et al. [17] noted that PPA dosages between 0.75% and 1.0% with 4% SBS balanced high-temperature stability with low-temperature flexibility, optimizing binder resistance under diverse climatic conditions. Pamplona et al. [18] further demonstrated that adding PPA improved recovery in the multi-stress creep recovery (MSCR) test and enhanced fatigue resistance in the linear amplitude sweep (LAS) test. These findings suggest that the combined use of SBS and PPA can address limitations associated with individual modifiers, offering a promising pathway for improving asphalt binder performance.

Despite these advances, there are still substantial gaps in understanding the combined effects of PPA and SBS on asphalt binders, particularly in terms of their microstructural behavior and chemical interactions. While previous studies have examined their performance at varying conditions, the mechanistic insights into how PPA structurally modifies SBS within the asphalt matrix remain underexplored. This study aims to fill this gap by investigating the progressive transformations in microstructure, phase interaction, and chemical composition across different PPA dosages. Furthermore, the temperature-dependent effects of PPA on asphalt properties, as noted by Pamplona et al. [18], underscore the necessity of dosage optimization to achieve a balanced performance across diverse conditions. A key aspect of this research is the integration of multi-criteria decision analysis to systematically correlate binder modifications with performance enhancements. The study comprehensively evaluates the synergistic effects of 3% SBS combined with varying PPA dosages (0.3%, 0.6%, and 0.9% by weight of asphalt cement) on binder properties through detailed physical, rheological, and chemical analyses.

The 3% SBS dosage, selected based on the average value used in Iraq, aligns with local industry practices for enhancing binder performance under high annual temperatures and increasing traffic loads [19,20]. The PPA used in this study has a 105% concentration of H_3PO_4, chosen to mitigate risks such as foaming during mixing with asphalt cement [4]. By integrating microstructural analysis with binder performance evaluations, this study aims to develop an optimized asphalt formulation capable of withstanding extreme temperatures and heavy traffic conditions.

2. Raw Materials

2.1. Asphalt Cement

The asphalt cement used in this study was obtained from the Doura refinery, located southwest of Baghdad. The physical properties of the asphalt cement, as shown in Table 1, comply with the penetration grade of 40/50 in the specification [21]. The rheological properties presented in Table 2 meet the Performance Grade (PG) 70-16 by the AASHTO M320 standards.

Table 1. Physical properties of asphalt cement.

Test	Unit	ASTM Designation	Result	Specification Limit [21]
Before the thin film oven test:				
Ductility	cm	ASTM D113	110	Min. 100
Flashpoint	°C	ASTM D92	297	Min. 232
Softening point, ring, and ball.	°C	ASTM D36	50.1	----
Specific gravity at 25 °C	----	ASTM D70	1.018	----
Penetration at 25 °C, 100 gm, and 5 s	0.1 mm	ASTM D5	49	40–50
Residue from thin film oven test (ASTM D1754):				
Ductility at 25 °C, 5 cm/min	cm	ASTM D113	60	Min. 25
Retained penetration, % of original	%	ASTM D5	62	Min. 55

Table 2. Rheological properties of asphalt cement.

Asphalt Cement	Properties	Temperature (°C)	Measurement	Specification (AASHTO M320-05)
Original	Flash Point (°C)	-	297	230 °C, min
	Viscosity at 135 °C (Pa.s)	-	741.2	3000 m Pa.s, max
	DSR, G/sinδ at 10 rad/s (kPa)	64	3.4962	1.00 kPa, min
		70	1.6266	
		76	0.8114	
RTFO Aged	Mass Loss (%)	-	0.271	1%, max
	DSR, G/sinδ at 10 rad/s (kPa)	64	7.1648	2.2 kPa, min
		70	3.1402	
		76	1.4623	
PAV Aged	DSR, G.sinδ at 10 rad/s (kPa)	28	3499	5000 kPa, max
		25	5204	
	BBR, Creep Stiffness (MPa)	−6	188	300 MPa, max
	Slope m-value	−6	0.371	0.3, min

2.2. Binder Modifiers (SBS and PPA)

SBS (commercial name, Kraton® D1192, Shanghai, China) is a linear block copolymer consisting of hard polystyrene (styrene) end blocks and a soft, elastic polybutadiene middle block [22,23], with a styrene content of 30% by mass. The properties of SBS are provided in Table 3. Polyphosphoric acid (PPA), supplied by CDH (P) Ltd., is a liquid inorganic compound with a H_3PO_4 equivalency of 105% and the chemical formula $H_{n+2}P_nO_{3n+1}$ [24]. The properties of PPA are summarized in Table 4. Figure 1 displays the physical state of the two binder modifiers.

Table 3. Properties of SBS.

Property	Measurement
Specific Gravity	0.94
Bulk Density (25 °C, g/cm³)	0.4
Hardness, Shore A (Measured on compression molded slabs)	70
Elongation at Break (%)	1000
Tensile Strength (MPa)	33
Solution Viscosity (Pa.s) (Measured on 25% mass solution in toluene at 25 °C)	1.8
Total Styrene Mass Content (%)	30
Ashes (%)	0.31

Table 4. Properties of PPA.

Property	Measurement
Physical State	Liquid
Appearance	Viscous liquid
Color	Colorless, clear
Odor	Odorless
Concentration of P_2O_5 (%)	85
Density at 25 °C (g/cm³)	1.93
Vapor Pressure at 25 °C (Pa)	2.66×10^{-6}
Surface Tension (N/cm)	79×10^{-5}
Specific Heat Capacity (J/g/°C)	1.549
Boiling Point (°C)	300
Viscosity at 25 °C (Pa.s)	0.84

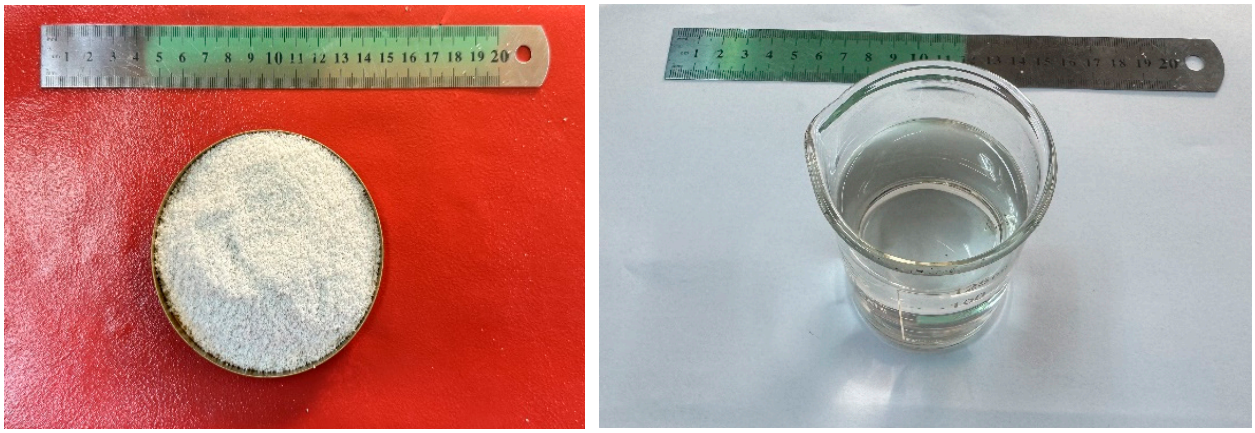

(**a**) SBS (**b**) PPA

Figure 1. Physical appearance of SBS and PPA.

2.3. Blend Preparation Method

The asphalt modification followed a systematic approach, as described by Wei et al. [17]. At first, the virgin asphalt was heated to 150 ± 1 °C until it was fully liquified. Thereafter, the pre-weighed SBS particles, 3% by weight of the asphalt cement, were gradually introduced into the asphalt at a rate of approximately 5 g/min and mixed using a Jiffy head high-speed shear mixer at 4500 rpm for 30 min. The pre-measured PPA was then added to the SBS-modified asphalt, and the mixture underwent additional high-speed shear mixing for another 30 min. Figure 2 illustrates the mixing instrument and proce-

dure. Finally, the prepared PPA and SBS-modified asphalt were poured into designated containers for storage and subsequent testing.

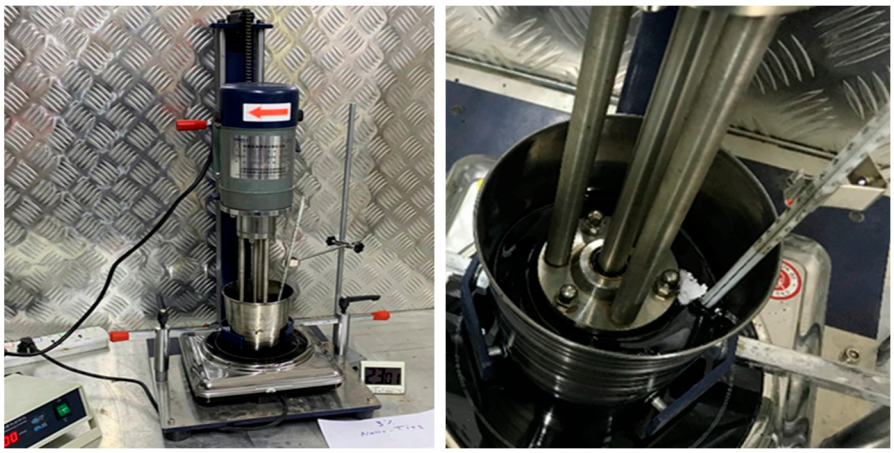

Figure 2. Binder blend preparation using a high-speed shear mixer.

3. Experimental Tests

The experimental methodology employed in this study is outlined in Figure 3, which shows all the tests conducted and the asphalt modification formulas.

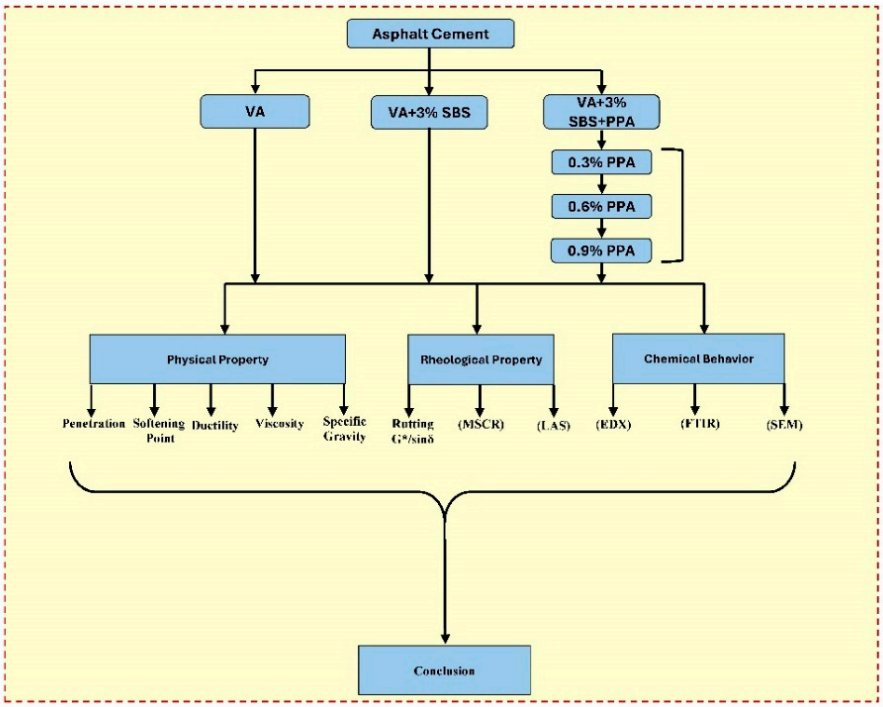

Figure 3. Overview of the experimental program.

3.1. Physical Tests

The penetration (at 25 °C) and softening point tests were conducted following ASTM D5 and ASTM D36 standards, respectively, to evaluate the stiffness and thermal susceptibility of the binders. The ductility test (at 25 °C) was performed following ASTM D113 to measure the tensile properties and the maximum deformation (elongation) capacity until break. Moreover, the rotational viscosity test (ASTM D4402) was used to evaluate the viscosity at 135 °C, reflecting the binders' workability. Also, the specific gravity was determined according to ASTM D70 to assess the influence of modification on volumetric properties.

3.2. Rheological Test

An oscillating shear test under high temperature was performed for unaged binders using a dynamic shear rheometer (DSR) (Anton Paar - SmartPave 102e, as shown in Figure 4). The testing procedure followed the AASHTO T315 standard, using a 25 mm diameter plate and keeping a gap of 1 mm between the plate and the specimen. While AASHTO T315 provides valuable insights into high-temperature performance, the low shear strain level under high temperature cannot fully reflect binder behavior under broad field conditions. To address this limitation, an additional multi-stress creep recovery (MSCR) test and linear amplitude sweep (LAS) test was also performed.

Figure 4. DSR-type SmartPave 102 e and testing specimens.

3.3. MSCR Test

The multi-stress creep recovery (MSCR) test was conducted in accordance with the AASHTO T350 standard to evaluate the resistance of the rolling thin film oven (RTFO)-conditioned asphalt binders to permanent deformation. The test was performed with DSR using a 25 mm parallel plate with a 1 mm gap. The temperature was set at the high PG temperature. The binder samples were subjected to a series of creep and recovery cycles at two stress levels, i.e., 0.1 kPa and 3.2 kPa. In the test, samples were first subjected to the 0.1 kPa stress for 20 cycles, followed by an additional 10 cycles under 3.2 kPa, resulting in 30 cycles. Each cycle consisted of 1 s creep loading (stress τ) and immediately following 9 s recovery (rest). In total, the test lasted for 300 s. Figure 5 illustrates an example of an MSCR test with three cycles of creeping stress of 0.1 kPa followed by another three cycles of creep stress of 3.2 kPa. From the recorded strain history, we can work out the peak strain (ε_p), recovered/elastic strain (ε_r), and non-recoverable/plastic strain (ε_{nr}) of each cycle. Three other parameters were employed to characterize the viscoelastic behavior of binders; they are the percent recovery (%R), non-recoverable creep compliance (J_{nr}), and stress sensitivity ($J_{nr,diff}$), in terms of the definition equations below (Equations (1)–(3)).

$$\%R = \frac{\varepsilon_r}{\varepsilon_p} \times 100 \quad (1)$$

$$J_{nr} = \frac{\varepsilon_{nr}}{\tau} \quad (2)$$

$$J_{nr} = \frac{\varepsilon_{nr}}{\tau} \quad (3)$$

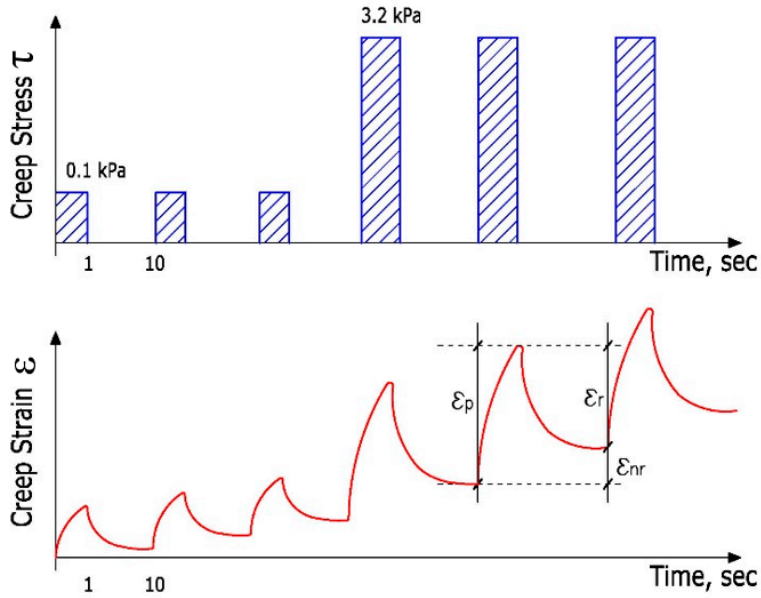

Figure 5. MSCR test loading scheme and typical output strain.

3.4. LAS Test

The linear amplitude sweep (LAS) test was conducted to evaluate the fatigue resistance of the modified asphalt binders under cyclic loading, following the AASHTO T391 standard. The test was performed using the dynamic shear rheometer (DSR) at the intermediate pavement temperature corresponding to the performance grade (PG) specified by AASHTO M320. The binder samples were aged using the rolling thin-film oven (RTFOT, AASHTO T240) and the pressure aging vessel (PAV, AASHTO R28) to simulate the aging in service. The test was conducted using 8 mm parallel plates with a gap of 2 mm, as recommended by AASHTO T315. The LAS test consists of two main stages: frequency sweep and amplitude sweep. In the frequency sweep stage, a repetitive shear load of a constant amplitude of 0.1% strain was applied across a range of frequencies from 0.2 to 30 Hz. The results were used to calculate the undamaged material property parameter, α. In the amplitude sweep stage, the repeated loads had a fixed frequency of 10 Hz, and meanwhile, the load amplitude increased linearly by controlling the strain from 0% to 30%, given the cycles up to 3100 at this test stage. Four key parameters—peak shear strain, peak shear stress, phase angle (δ), and dynamic shear modulus (G*)—were recorded at a regular interval, 10 cycles, in both stages. The viscoelastic continuum damage (VECD) model was applied to interpret the LAS test results and predict fatigue life (N_f, as shown in Equation (4)) [25,26].

$$N_f = A(\gamma_{max})^{-B} \quad (4)$$

where γ_{max} represents the maximum expected strain on the pavement, A indicates the damage characteristics of the binder, and B describes the undamaged binder property determined through amplitude sweep and frequency sweep tests, respectively.

3.5. Microstructure and Chemical Composition Tests

Scanning Electron Microscopy (SEM), Energy Dispersive X-ray Spectroscopy (EDX), and Fourier-Transform Infrared Spectroscopy (FTIR) were utilized to analyze the microstructural and compositional characteristics. Figure 6 shows the instruments. FTIR

analysis was carried out using a BRUKER Alpha II device. SEM analysis was conducted at a magnification level of 30,000.

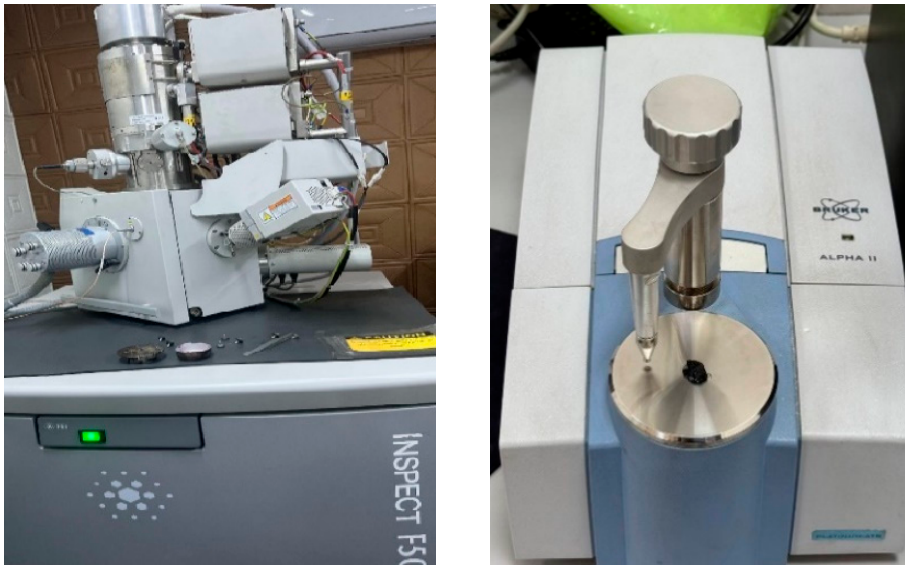

Figure 6. Instruments for microstructure and composition analysis.

4. Results and Discussion

4.1. Physical Properties

Figures 7–11 illustrate the physical properties of the tested asphalt binders. Figure 7 shows that 3% SBS alone significantly reduces the penetration resistance by 30.61% of the virgin asphalt binder (VA). Penetration further decreases with the addition of PPA, with the PPA content increasing from 0.3% to 0.6% and then to 0.9%, but with a gradual slowed reduction rate. The results indicate that both SBS and PPA help improve the stiffness of binders, which agrees with what Li et al. [16] and Niu et al. [27] reported, where both studies used softer grade asphalt (60/70) and different percentages of SBS and PPA. Figure 8 compares the softening point of binders, which shows an opposite trend to that in Figure 7, where the 3% SBS addition gives a 14.17% increase in the softening point of the VA. With the extra addition of the PPA, the softening point further increases with the increase in the content of the PPA from 0.3 to 0.6 to 0.9%, but the rate of increase gradually slows down. The results demonstrate that both SBS and PPA help enhance the thermal stability of the binder. The results are comparable with those reported by Wei et al. [17], who used two different penetration grades (60/70) and (80/90) asphalt and various percentages of SBS and PPA. Figure 9 shows the measured ductility, where it can be seen that the addition of 3% SBS alone increases flexibility by 18.18%. However, the PPA causes ductility to decrease with its added content. The result is aligned with what was observed by Li et al. [16] and Niu et al. [27], who conducted their tests at a lower temperature of 5 °C. Figure 10 compares the measured rotational viscosity, where the results present a similar trend as that of the penetration in Figure 7. The 3% SBS addition increases the viscosity by 110.47% of the VA. The PPA addition generated a further increase of the viscosity in an approximately linear trend with its added content but at a slowed-down rate. The result is consistent with that reported by Hossain et al. [28] and Niu et al. [27]. Figure 11 compares the specific gravity of all investigated binders, showing that SBS and PPA addition increases the density of binders.

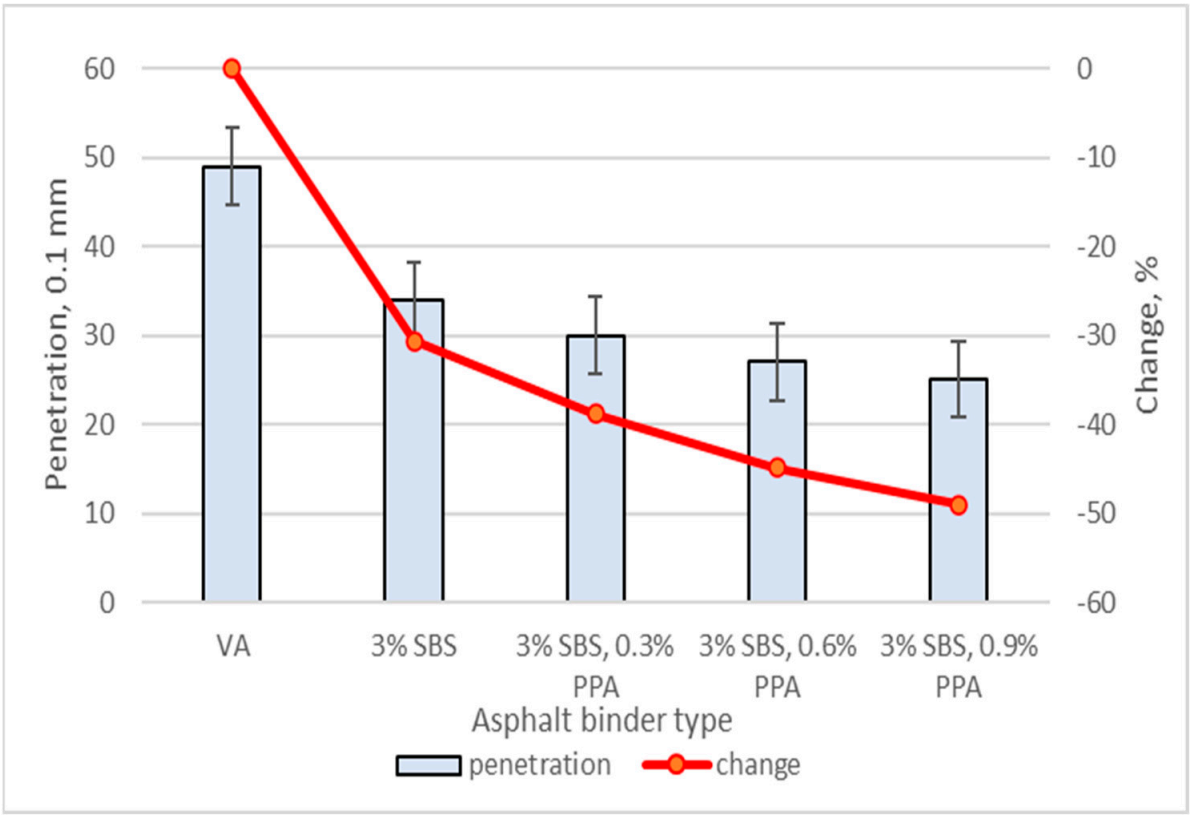

Figure 7. Variations in penetration results.

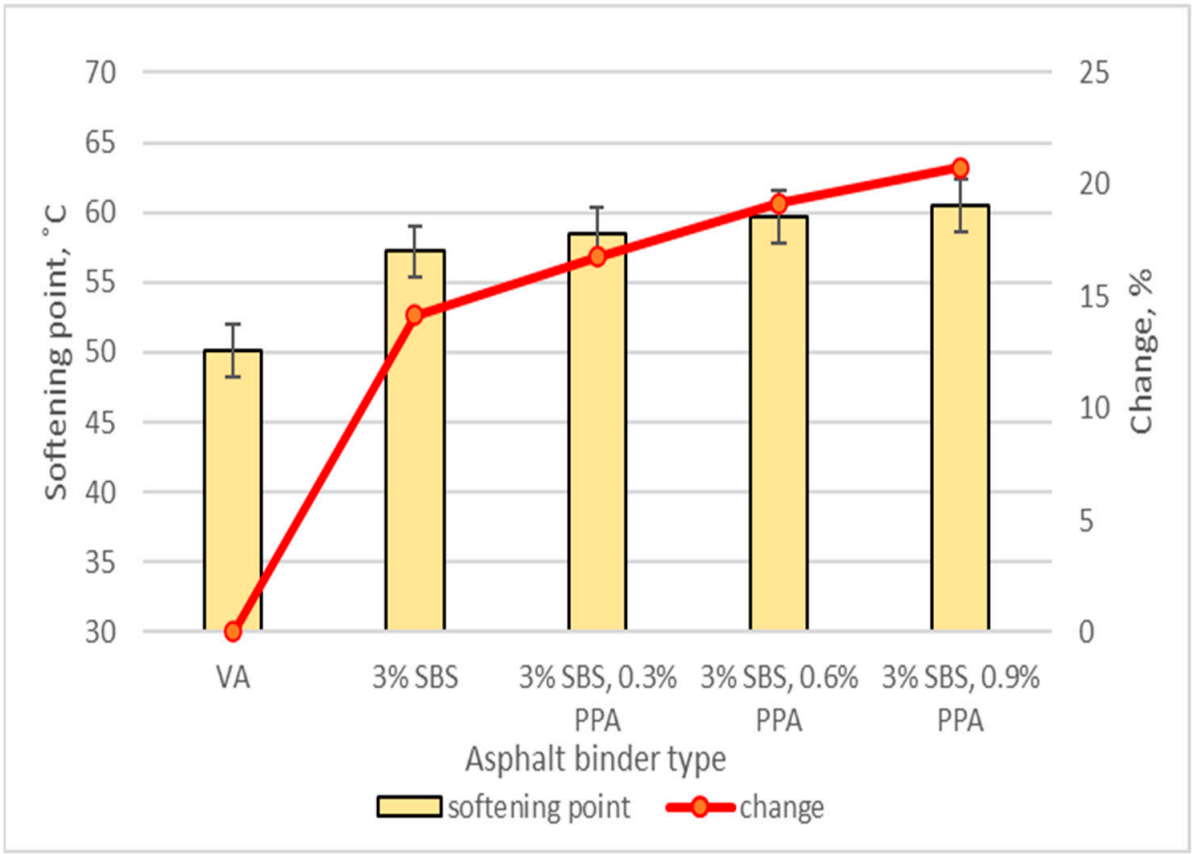

Figure 8. Variations in softening point results.

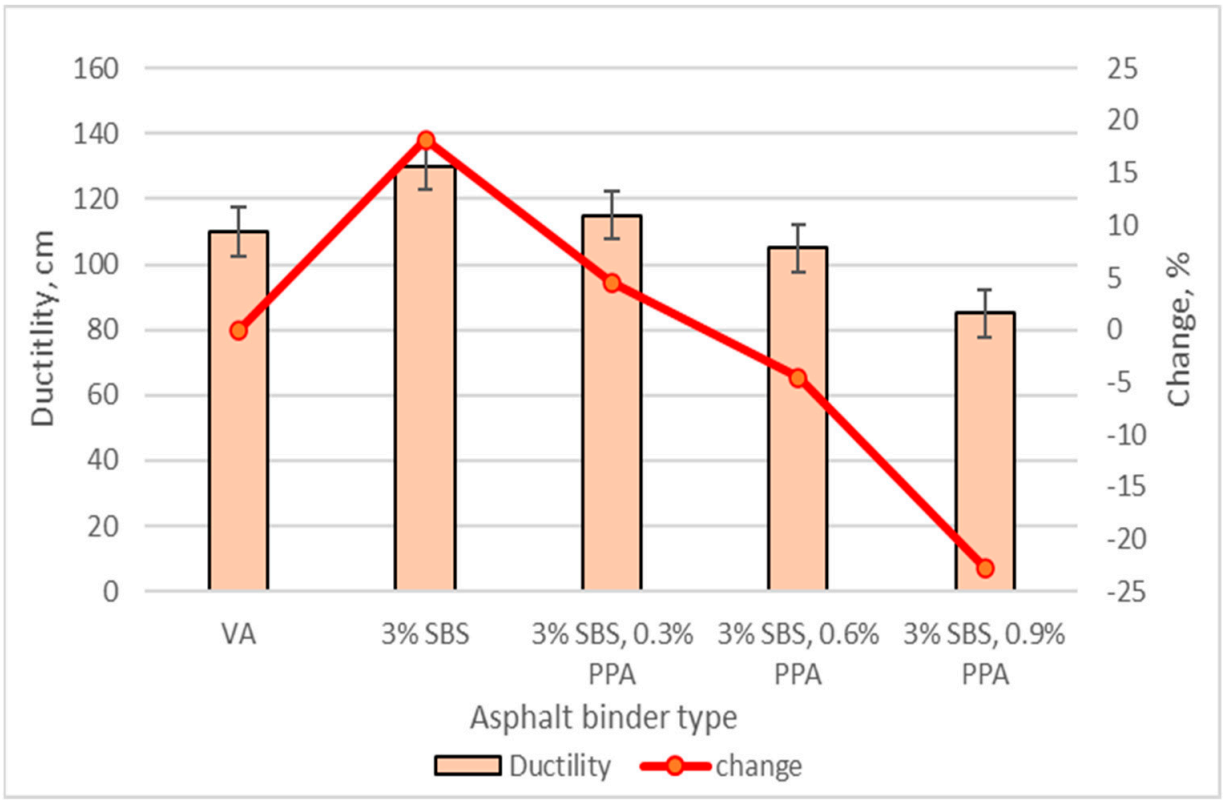

Figure 9. Variations in ductility results.

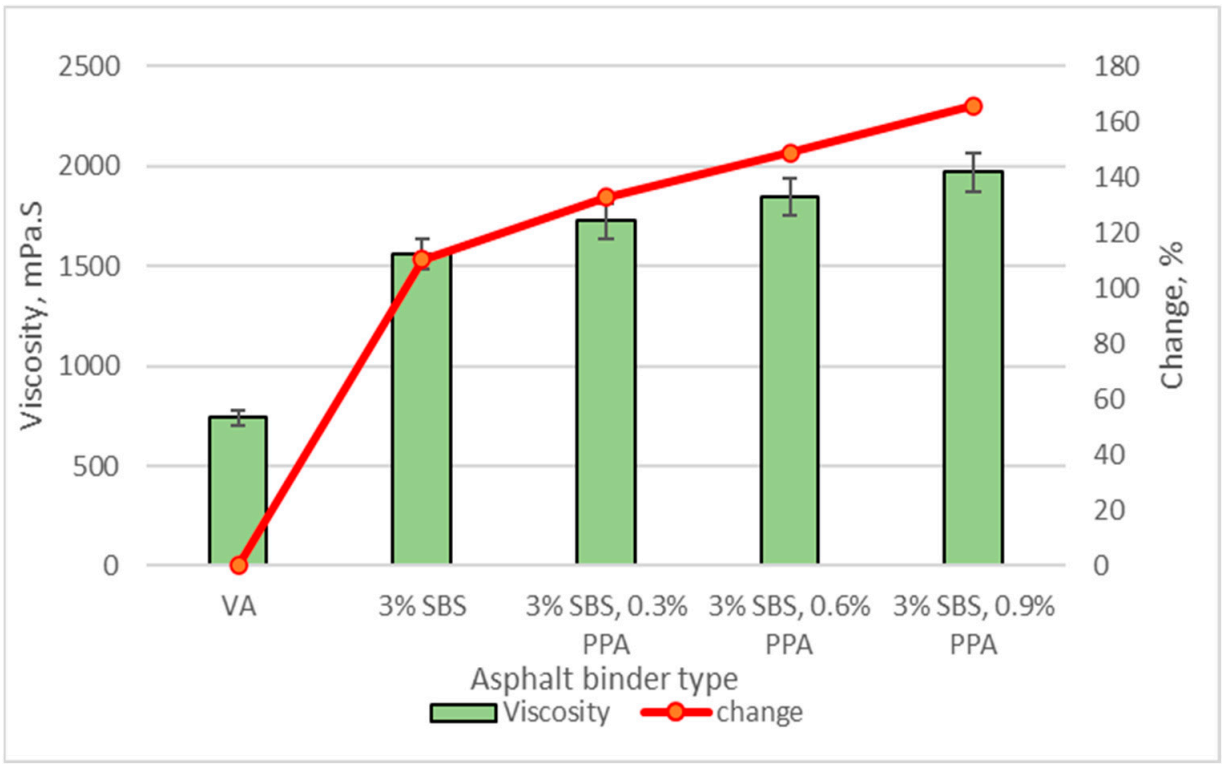

Figure 10. Variations in viscosity results.

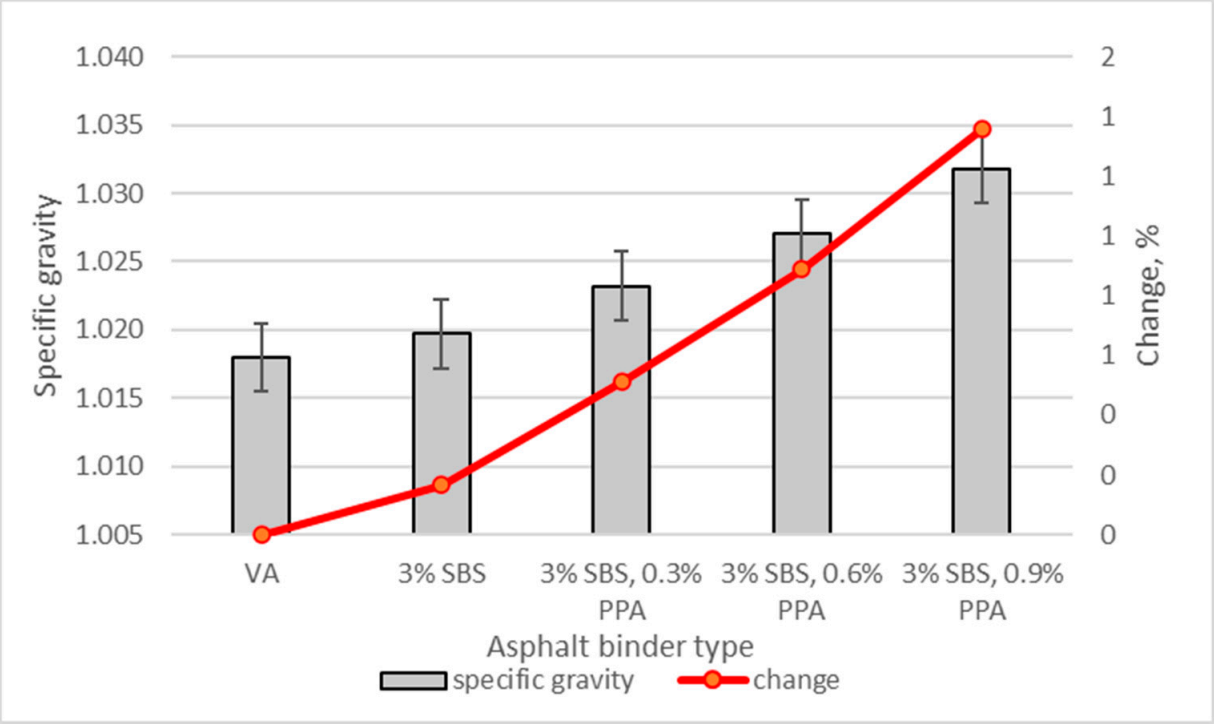

Figure 11. Variations in specific gravity results.

4.2. Rheological Properties

Figure 12 presents the variations in two rheological properties, complex shear modulus (G*) and phase angle (δ), for all binders over a temperature range from 58 °C to 94 °C. The results show that adding 3% SBS significantly enhances the virgin asphalt (VA) stiffness, particularly at lower temperatures, where an increase in G* is observed compared to VA. However, at temperatures above approximately 80 °C, the effect of SBS alone diminishes, indicating that while SBS enhances elasticity and stiffness, its effect is temperature-dependent. The incorporation of PPA further improves the high-temperature performance of the SBS-modified binders. The G* values increase progressively with increasing PPA content (0.3%, 0.6%, and 0.9%), demonstrating improved stiffness and resistance to deformation. Notably, the binder modified with 3% SBS and 0.9% PPA exhibits the highest G* values across all tested temperatures, suggesting that the combination of SBS and PPA provides a more thermally stable binder. However, the temperature sensitivity of the modified binders varies, with VA showing the steepest decline in G*, indicating lower resistance to temperature-induced softening. In contrast, SBS-modified binders with PPA maintain higher G* values over a broader temperature range, confirming the ability of PPA to enhance stiffness while stabilizing the binder at elevated temperatures.

The phase angle (δ) trends in Figure 12 further support the stiffening effect of SBS and PPA. A lower δ value indicates a more elastic response, which improves rutting resistance. Adding 3% SBS reduces δ compared to VA, signifying increased elasticity. Moreover, incorporating PPA further decreases δ, particularly at lower temperatures, reinforcing the positive influence of PPA in improving the elastic response of the binder. The binder modified with 3% SBS and 0.9% PPA exhibits the lowest δ values across the temperature range, confirming that higher PPA dosages contribute to enhanced elastic behavior and delayed softening.

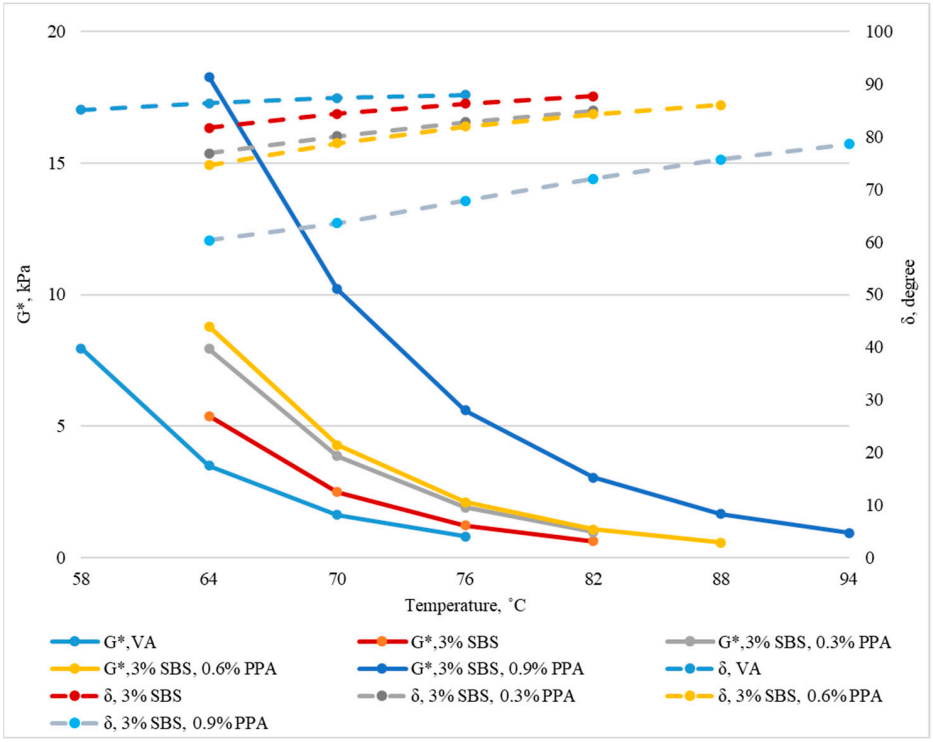

Figure 12. Variations in the rheological properties G* and δ with temperature.

Figure 13 compares the binders' calculated rutting factor (G*/sin δ). The G*/sin δ curves present a similar pattern as that of the G* curves in Figure 12. The binder VA exhibits the lowest rutting resistance, which fails to meet the AASHTO M320 criterion of 1 kPa at higher temperatures. In contrast, all the binders modified with 3% SBS and different PPA percentages have improved higher G*/sin δ values at specific temperatures. Notably, the results indicate that the binder with 3% SBS and 0.9% PPA improved the rutting resistance compared with all other binders. It is also observed that the effective temperature range extends when using the 3% SBS with an increasing content of PPA. The results are consistent with the findings of other researchers (Li et al. [16], Wei et al. [17], Hossain et al. [28], and Rossi et al. [5]).

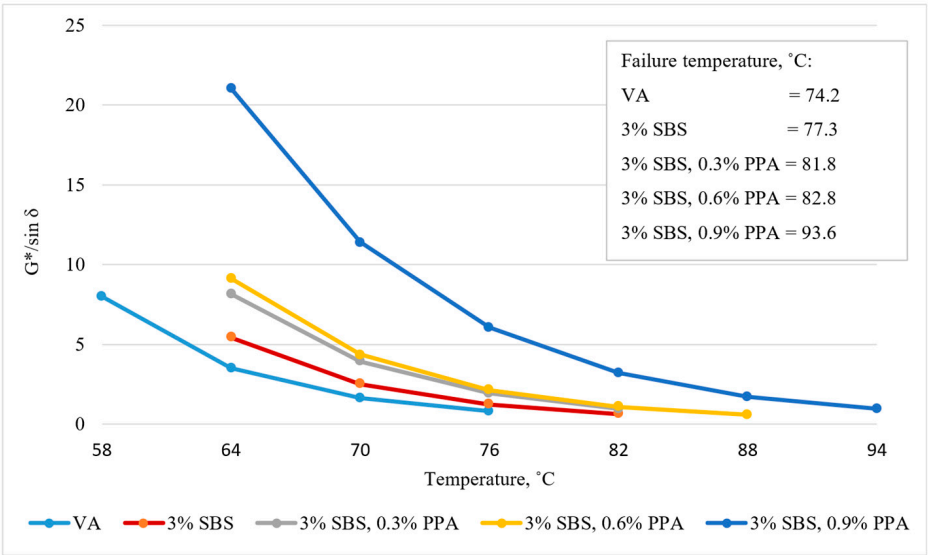

Figure 13. G*/sin δ variations with temperature and true fail temperatures.

4.3. MSCR Results

Per the Superpave requirements, the MSCR test was conducted at 76 °C, corresponding to the anticipated average 7-day maximum pavement temperature. Table 5 lists the parametric results. It can be noticed that the non-recoverable creep compliance parameter, J_{nr}, at both stress levels, 0.1 kPa and 3.2 kPa, decreases with the addition of modifiers and the increase in the PPA content. Notably, the binder presents a significant decrease in the J_{nr} values when PPA content increases from 0.6% to 0.9%. The lower the J_{nr} magnitude, the better the rutting resistance. The stress sensitivity, $J_{nr,diff}$ results also indicate that the modifiers make the binder less sensitive to the applied load, i.e., the lower the $J_{nr,dif}$ the less the J_{rn} difference under different loads. The elastic recovery percentage (%R) represents the proportion of strain recovered after unloading. The results show that the binder of 3% SBS and a higher PPA content possesses better elasticity. This characteristic is attributed to the elastic property and molecular crosslink network of the SBS block in the modified binder [29]. Meanwhile, adding PPA further improves the SBS block elasticity due to the synergistic reactions between the two modifiers. Table 6 lists the grade classification of binders and the specification in AASHTO M332. Referring to Tables 5 and 6, the 3% SBS and 0.9% PPA binder can be classified as grade V, a high grade that meets the demands for high-temperature and heavy-load applications, while the VA binder fails to meet the lowest grade, S.

Table 5. MSCR parametric indices.

Asphalt Binder	$J_{nr\_0.1kPa}$ (kPa^{-1})	$J_{nr\_3.2kPa}$ (kPa^{-1})	$J_{nr,diff}$ (%)	$\%R_{3.2}$ (%)
VA	3.3108	5.4661	65.1	0.22
3% SBS	3.1232	4.1976	34.4	0.57
3% SBS, 0.3% PPA	2.6378	3.4761	31.78	1.32
3% SBS, 0.6% PPA	2.4073	2.9906	24.23	3.55
3% SBS, 0.9% PPA	0.7049	0.8508	20.7	15.6

Table 6. AASHTO M332 pavement asphalt grades.

Paving Grade	Test Temperature	Requirements
S	PG high temperature	$J_{nr\_3.2kPa} \leq 4.5.0$ kPa, % $R_{3.2kPa} \leq 75\%$
H	PG high temperature	$J_{nr\_3.2kPa} \leq 2.0$ kPa, % $R_{3.2kPa} \leq 75\%$
V	PG high temperature	$J_{nr\_3.2kPa} \leq 1.0$ kPa, % $R_{3.2kPa} \leq 75\%$
E	PG high temperature	$J_{nr\_3.2kPa} \leq 0.5$ kPa, % $R_{3.2kPa} \leq 75\%$

Figure 14 shows the accumulated permanent strain through the MSCR tests. It can be seen that the binder modifiers helped reduce the accumulated permanent deformation, particularly the binder of 3% SBS and 0.9% PPA, which stands away with much-reduced permanent deformation at all stages throughout the whole process. Moreover, all the MSCR test results are in agreement with the findings by Cao et al. [30] and Rani et al. [31].

4.4. LAS Results

The fatigue resistance of the asphalt binders was assessed through LAS testing conducted at 16 °C, an intermediate temperature condition. Figure 15 illustrates the tested binders' effective shear stress versus effective strain curves. The strain level at peak stress serves as an indicator of material flexibility. The higher the strain levels, the more excellent the resistance to fatigue damage. Additionally, the flatter the curve's post-peak slope, the more minor the accumulated fatigue damage. The results indicate that the SBS binder with 0.9% PPA has the highest effective shear stress. However, the SBS binder with 0.6% PPA

shows the least accumulated fatigue damage. In general, all modified binders outperformed the VA binder in terms of fatigue resistance and level of damage.

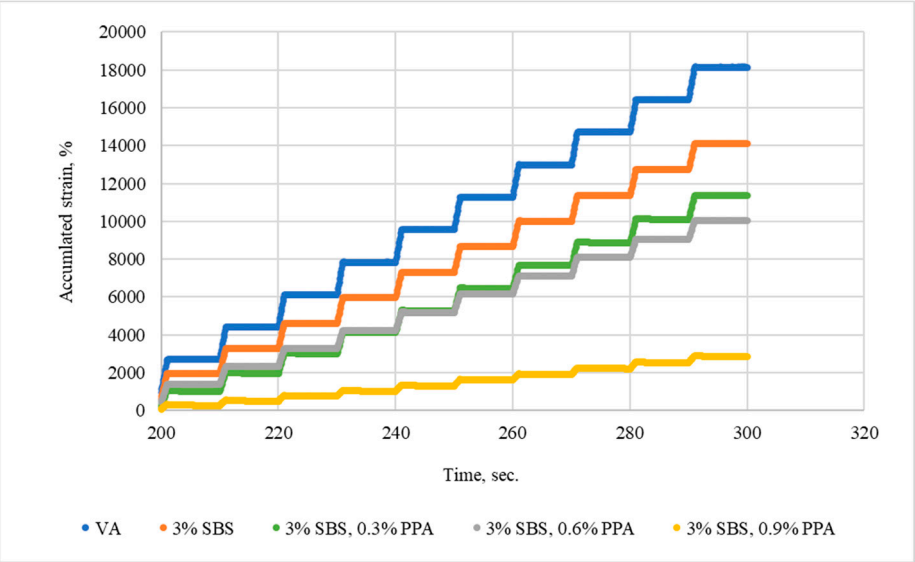

Figure 14. Accumulated strain vs. time curves for different asphalt binders.

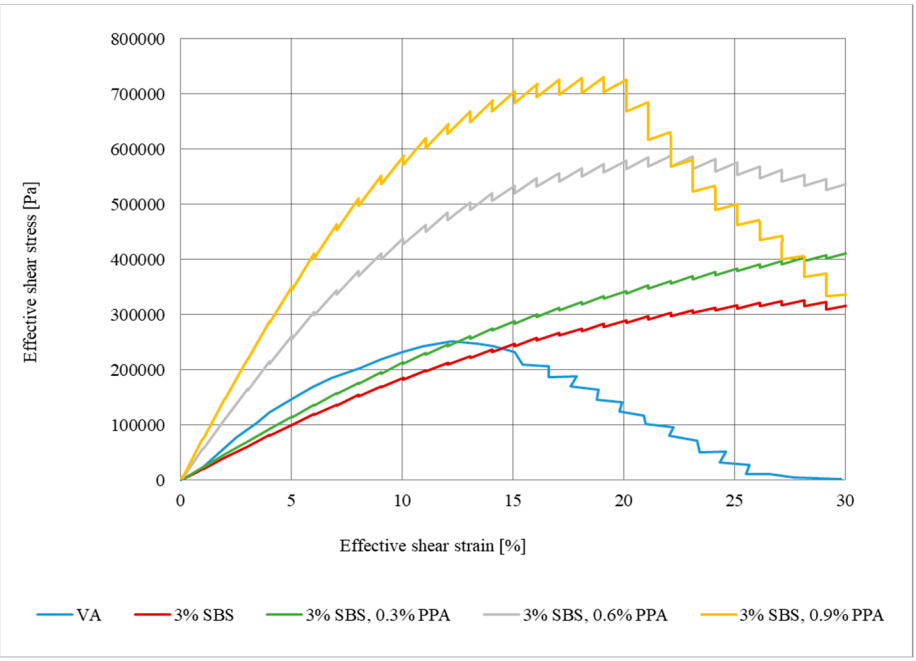

Figure 15. Effective stress vs. effective strain relationship for varying asphalt types.

The LAS results were further analyzed using the viscoelastic continuum damage (VECD) model, which effectively models the complex fatigue behavior of asphalt binders. Figure 16 illustrates the estimated fatigue life (N_f) vs the strain (γ) as calculated by Equation (4). Table 7 compares the calculated fatigue life at two strain states, i.e., 2.5% and 5%, which reflects two pavement thickness situations, i.e., thick and thin, respectively. The results show that the VA binder has the lowest fatigue life, while the SBS binder of 0.3% PPA achieved the highest fatigue of the two strains.

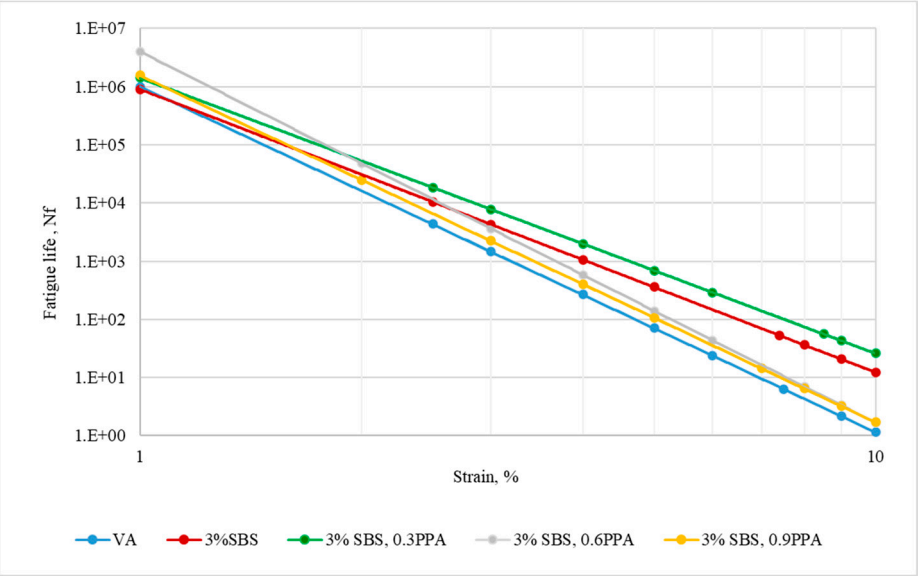

Figure 16. Fatigue life for varying binder types.

Table 7. Fatigue life at two strain states.

Binder Type	Strain Level (%)	N_f
VA	2.5	4333
	5.0	71
3% SBS	2.5	10,459
	5.0	358
3% SBS, 0.3PPA	2.5	18,481
	5.0	694
3% SBS, 0.6PPA	2.5	11,704
	5.0	141
3% SBS, 0.9PPA	2.5	6639
	5.0	107

The decline in the binder's fatigue life at higher PPA dosages (0.6% and 0.9%) may be explained by the fact that excessive PPA beyond 0.3% enhances stiffness, which trades off flexibility to withstand repetitive cyclic loading. These findings are consistent with previous similar studies [27,28] of other percentages.

4.5. Microstructure and Chemical Composition Analyses

4.5.1. EDX Analysis

The EDX analysis results are summarized in Table 8. The analysis focused on the key elements, carbon (C), sulfur (S), oxygen (O), and phosphorus (P), to highlight the chemical changes induced by the addition of SBS and PPA modifiers. The VA binder exhibits a high carbon content (91 at.%, 79.16 wt.%), aligning with its hydrocarbon characteristic. It also has a higher sulfur content (7.3% at.%, 17.14% wt.%). In addition, a small amount of trace elements, such as aluminum (Al) and calcium (Ca), was also observed. With the incorporation of 3% SBS, the carbon atomic content slightly decreased to 89%, reflecting the partial replacement of hydrocarbons by the polymeric modifier. Oxygen content increased slightly (2% at.%, 2.62% wt.%), likely introduced by the SBS composition. Significantly, sulfur atomic content slightly decreased to 7% (18.21 wt.%), indicating minor chemical interactions between the sulfur compounds in the binder and SBS.

Table 8. EDX elemental composition of asphalt.

Sample	Element	at.%	at.% Error	wt.%	wt.% Error
VA	C	91.00	0.60	79.16	0.52
	Al	1.10	0.00	2.27	0.00
	S	7.30	0.10	17.14	0.23
	Ca	0.50	0.00	1.43	0.00
3% SBS	C	89.00	0.60	77.31	0.52
	O	2.00	0.10	2.62	0.13
	S	7.00	0.10	18.21	0.26
	Ni	0.20	0.00	1.86	0.10
3% SBS 0.3% PPA	C	90.47	0.60	77.03	0.53
	O	2.50	0.10	3.29	0.13
	S	6.90	0.10	16.80	0.25
	P	0.13	0.05	0.95	0.10
3% SBS 0.6% PPA	C	89.22	0.04	76.10	0.53
	O	4.00	0.10	5.22	0.13
	S	6.60	0.10	16.06	0.25
	P	0.18	0.06	1.31	0.12
3% SBS 0.9% PPA	C	88.64	0.60	75.22	0.53
	O	5.10	0.10	6.48	0.13
	S	6.00	0.10	15.29	0.25
	P	0.26	0.05	1.88	0.15

Including PPA alongside SBS led to further elemental changes, with an increase in the phosphorus (P) content, reflecting the presence of PPA. The phosphorus content increased progressively with higher PPA dosages, from 0.13 at.%(0.95 wt.%) at 0.3% PPA to 0.26 at.% (1.88 wt.%) at 0.9% PPA. Simultaneously, oxygen content also increased proportionally, reaching 5.1 at.% (6.48 wt.%) at the highest PPA dosage. This trend indicates increased oxidation within the binder, likely due to chemical interactions between PPA and the matrix. The sulfur content decreased gradually with the addition of PPA, dropping from 7 at.%(18.21 wt.%) in the 3% SBS sample to 6 at.%(15.29 wt.%) in the binder modified with 3% SBS and 0.9% PPA. This reduction suggests a redistribution or potential chemical reaction involving sulfur during the modification process, which could contribute to improved thermal and chemical stability.

The progressive increase in oxygen and phosphorus contents with higher PPA dosages reflects the chemical contributions of PPA, which enhances oxidative stability and chemical interaction within the binder matrix. The reduction in sulfur content with PPA addition may indicate a shift in the binder's chemical equilibrium, potentially enhancing its durability under varying service conditions.

4.5.2. FTIR Results Analysis

The FTIR results, presented in Figure 17, provide valuable insights into the molecular transformations occurring in asphalt binder upon modification with SBS and PPA. The analysis is divided into five key zones based on wavenumber ranges. In Zone 1 (3200–3700 cm^{-1}), the hydroxyl (O–H) stretching region, a broad absorption band appears around 3430 cm^{-1}, indicating the presence of hydroxyl or hydrogen-bonded functional groups. This peak is relatively weak in VA, but with the addition of SBS, a slight increase in intensity is observed, suggesting minor moisture absorption or weak hydrogen bonding interactions introduced by the polymer. As PPA is incorporated, the peak becomes more pronounced, particularly at 0.6% and 0.9% PPA, indicating a higher presence of phosphoryl-related

functional groups (P=O) or hydroxyl functionalities generated through oxidation and esterification reactions.

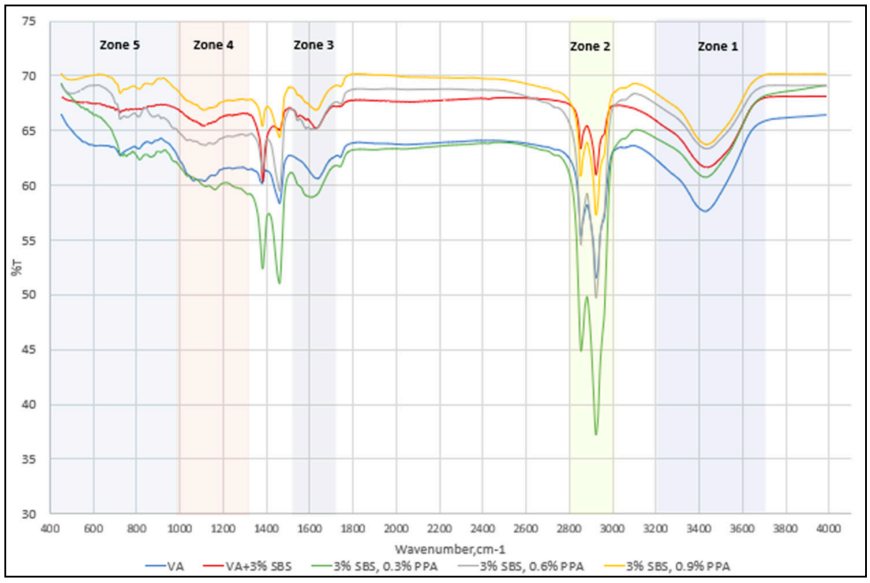

Figure 17. FTIR results for studied binders.

In Zone 2 (2800–3000 cm^{-1}), aliphatic C–H stretching vibrations dominate, with two primary peaks at 2924 cm^{-1} (CH_2 asymmetric stretch) and 2853 cm^{-1} (CH_3 symmetric stretch). These peaks are strong in VA and become more intense with SBS modification, confirming the increased presence of aliphatic hydrocarbon chains contributed by the polymer. However, when PPA is introduced, a gradual reduction in peak intensity is observed, particularly at 0.6% and 0.9% PPA, suggesting chemical modifications in the aliphatic structure, likely due to oxidation or polymer interactions. In Zone 3 (1550–1750 cm^{-1}), which includes carbonyl (C=O) and aromatic (C=C) stretching vibrations, significant changes occur. The C=O stretching peak at 1702 cm^{-1}, which is relatively weak in VA, increases in intensity upon SBS addition, indicating oxidation effects or potential interactions between the polymer and binder. As PPA content rises (0.3%, 0.6%, and 0.9%), this peak intensifies further, suggesting the formation of ester bonds due to esterification reactions promoted by PPA. Meanwhile, the C=C stretching peak at 1623 cm^{-1}, associated with the aromatic rings of asphalt, exhibits slight reductions in intensity with PPA modification, indicating potential interactions with the aromatic structure. In Zone 4 (1000–1350 cm^{-1}), the peaks correspond to sulfate (SO_2), phosphate (P=O), and ester (C–O–C) functionalities. The P=O stretching peak at 1311 cm^{-1}, absent in VA, appears and becomes increasingly pronounced with PPA addition, confirming the incorporation of phosphate groups. Additionally, the C–O–C and S–C stretching peaks around 1160 cm^{-1} show noticeable intensity increases, suggesting esterification reactions and the formation of sulfonated compounds, which modify the binder's chemical structure.

In Zone 5 (below 1000 cm^{-1}), characteristic peaks associated with polymeric structures and functionalized asphalt components are present. The butadiene peak at 966 cm^{-1}, which appears prominently in SBS-modified asphalt, confirms the presence of polymer units. However, as PPA content increases, this peak decreases in intensity, suggesting possible interactions between PPA and butadiene units, leading to structural modifications or polymer degradation. The styrene-related peaks at 874 cm^{-1} and 750 cm^{-1} also exhibit intensity reductions, indicating potential alterations in the SBS polymer backbone due to PPA addition.

4.5.3. SEM Analysis

Figure 18 presents the SEM micrographs of all binders at a magnification of 30,000, highlighting the microstructural evolution induced by SBS and PPA modification. The VA binder (Figure 18a) exhibits a smooth and uniform matrix, indicative of its homogeneous nature and minimal structural complexity. However, with the incorporation of 3% SBS (Figure 18b), the binder's microstructure becomes heterogeneous, with dispersed polymeric domains forming an irregular, foam-like network. This microstructural transformation is associated with the partial phase separation of SBS within the asphalt, contributing to enhanced elasticity and improved deformation resistance.

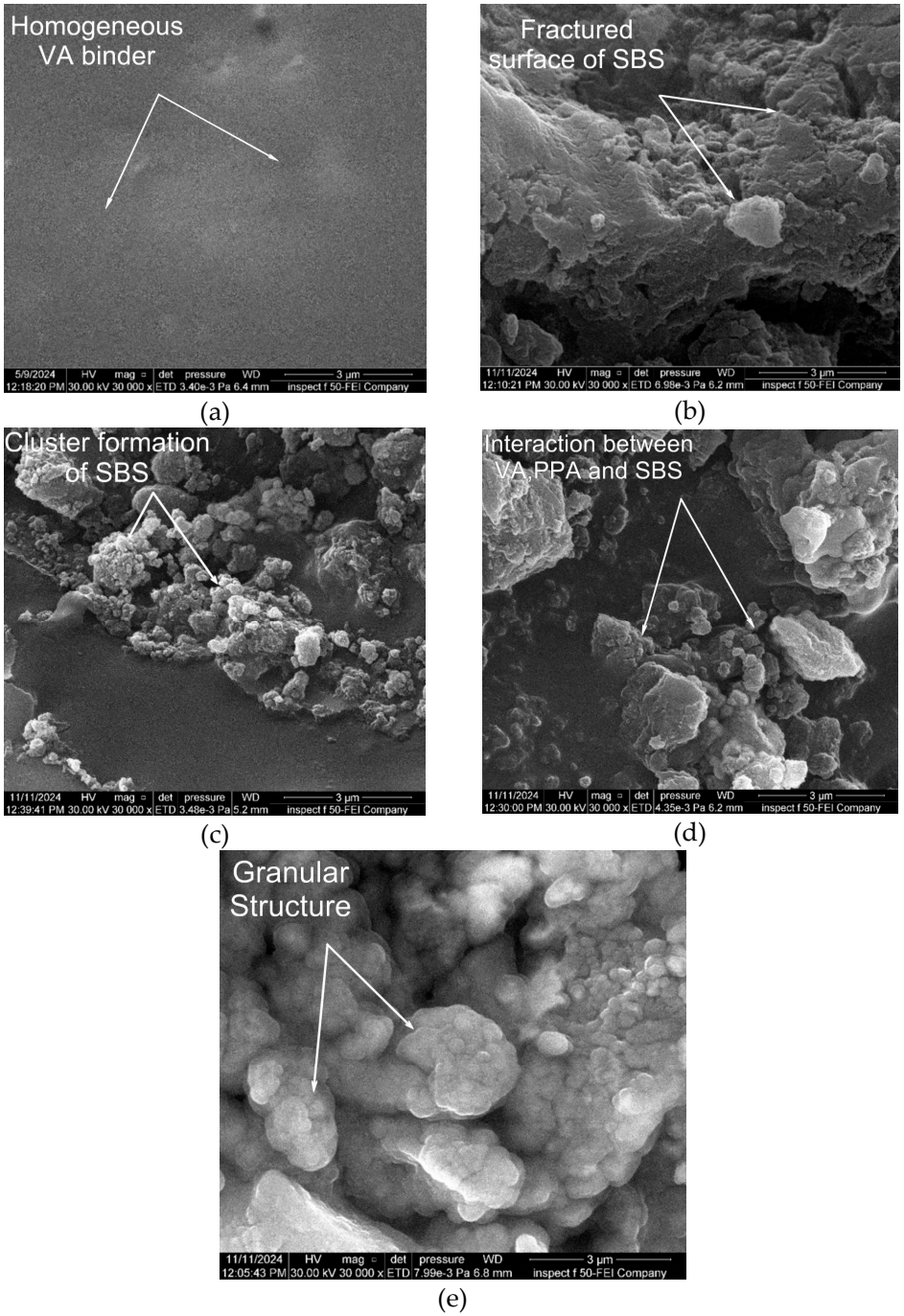

Figure 18. SEM images of: (**a**) AV, (**b**) 3% SBS, (**c**) 3% SBS + 0.3% PPA, (**d**) 3% SBS + 0.6% PPA, and (**e**) 3% SBS + 0.9% PPA.

Upon the addition of PPA, significant structural changes are observed. At 0.3% PPA (Figure 18c), the polymeric domains become more fragmented and granular, suggesting that PPA interacts with the SBS-modified binder by breaking down the foam-like network into smaller, well-distributed polymeric clusters. This transformation aligns with the known reaction mechanisms of PPA with asphalt functional groups, which enhance polymer dispersion and binder stability. As the PPA content increases to 0.6% and 0.9% (Figure 18d,e), the granular structures become progressively more compact, crosslinked, and homogeneous. At 0.9% PPA, the polymer-modified binder forms densely packed, agglomerated structures, signifying stronger chemical interactions between PPA, SBS, and the asphalt matrix. This agglomeration likely results from the acid-induced reorganization of asphaltenes and resins, promoting binder stiffness and rutting resistance. However, excessive PPA content may increase localized rigidity, potentially affecting the flexibility and fatigue resistance of the binder. These findings confirm that PPA not only alters the dispersion of SBS within asphalt but also modifies the binder's microstructural organization, reinforcing its resistance to high-temperature deformation. The observed granular refinement and structural densification further support the hypothesis that PPA enhances the chemical interaction between SBS and the asphalt matrix, contributing to improved performance properties.

5. Overall Desirability Analysis

Overall Desirability (OD) is a multi-criteria decision analysis method used to ascertain optimal resolution against multiple objectives [32]. This study applied OD analysis to evaluate and determine the most effective PPA level working with 3% SBS on the VA modification. The analysis considers a range of criterial properties (X): penetration (X_1), softening point (X_2), ductility (X_3), the temperature for the unit rutting index (G*/sin δ = 1 kPa) (X_4), the non-recoverable creep compliance at 3.2 kPa ($J_{nr\_3.2kPa}$) (X_5), percentage of recovery (%R) (X_6), and the number of fatigue cycles to reach 2.5% strain (N_f) (X_7). The OD parameters can be normalized by either of two different approaches, i.e., the "larger-the-better" following Equation (5) or the "smaller-the-better" following Equation (6).

$$x_i^*(k) = \frac{x_i(k) - minx_i}{maxx_i - minx_i} \tag{5}$$

$$x_i^*(k) = \frac{maxx_i - x_i(k)}{maxx_i - minx_i} \tag{6}$$

where i = 1, 2, …, m stands for the parameter i_d, m is the total number of the criterial parameters; k = 1, 2, …, n stands for the modification i_d, n is the total number of the binder modification types; $maxx_i$ is the maximum value of the i^{th} parameter of all the binders from VA to SBS and PPA modifications, and $minx_i$ is the minimum value of the i^{th} parameter of all binders.

Finally, the OD score is calculated in terms of Equation (7) for each modification type or binder type:

$$\gamma_{OD}(k) = [x_1^*(k)x_1^*(k) \ldots..x_m^*(k)]^{1/m} \tag{7}$$

The higher the OD score, the more desirable the combination of all properties. Table 9 shows the OD parametric values and calculated OD scores. It is evident that the asphalt binder modified with 3% SBS and 0.3% PPA achieves the highest OD score, reflecting superior overall balanced performance characteristics across the evaluated indices.

Table 9. The original normalized values and OD of asphalt binders.

Test Parameter	Binder Type	VA	3% SBS	3% SBS, 0.3% PPA	3% SBS, 0.6% PPA	3% SBS, 0.9% PPA
Penetration, X_1 (1/10 mm)	Original Value (P)	49	34	30	27	25
	Normalized Value (X_1*)	0.000	0.625	0.792	0.917	1.000
Softening point, X_2 (°C)	Original Value (SP)	50.1	57.2	58.5	59.7	60.5
	Normalized Value (X_2*)	0.000	0.683	0.808	0.923	1.000
Ductility, X_3 (cm)	Original Value	110	130	115	105	85
	Normalized Value (X_3*)	0.556	1.000	0.667	0.444	0.000
Rutting temp, X_4 (°C)	Original Value	74.2	70.7	75.3	71.1	69.3
	Normalized Value (X_4*)	0.817	0.233	1.000	0.300	0.000
Jnr, X_5 (kPa^{-1})	Original Value	5.4661	4.1976	3.4761	2.9906	0.8508
	Normalized Value (X_5*)	0.000	0.275	0.431	0.536	1.000
% Recovery, X_6 (%R)	Original Value	0.22	0.57	1.32	3.55	15.6
	Normalized Value (X_6*)	0	0.023	0.072	0.217	1
Fatigue life, X_7 (N_f, Cycles)	Original Value	4333	10459	18481	11704	6639
	Normalized Value (X_7*)	0	0.433	1	0.521	0.163
Overall Desirability (OD)		**0**	**0.309**	**0.539**	**0.49**	**0**

6. Conclusions

From the comprehensive reported study, the following main conclusions can be drawn from what has been found:

1. This study provides new insights into the combined effects of SBS and PPA on the physical properties of asphalt binders. While SBS alone enhances stiffness, adding PPA further modifies the binder structure, resulting in a 20.8% increase in softening point and a 48.9% reduction in penetration at 0.9% PPA. However, excessive PPA content negatively impacted ductility, emphasizing the need for an optimized balance to maintain flexibility.
2. The MSCR test demonstrated that the synergistic effect of SBS and PPA significantly enhanced the binder's rutting resistance, with $J_{nr3.2}$ reduced by 84.4% at 0.9% PPA, a far greater improvement than SBS alone. Notably, the elastic recovery (%R) increased by 70-fold compared to VA, confirming the modification's effectiveness in high-traffic applications. Unlike previous studies, this work quantitatively correlates the dosage-dependent response of PPA on rutting performance, providing a refined approach to binder optimization.
3. The LAS test revealed a 326% increase in fatigue life (N_f) at 0.3% PPA but a reduction at 0.9%, demonstrating that excessive PPA may compromise fatigue resistance. These findings highlight the trade-off between high-temperature performance and long-term durability.
4. EDX analysis confirmed an increase in oxygen and phosphorus content with higher PPA dosages, reflecting chemical modifications to the binder matrix. For instance, oxygen content rose from 2% with 3% SBS to 5.1% with 0.9% PPA, while phosphorus content increased from 0.13% at 0.3% PPA to 0.26% at 0.9% PPA. FTIR spectra indicated the formation of new functional groups, such as P=O bonds, highlighting improved rheological properties through chemical interactions.
5. The SEM analysis demonstrated the microstructural evolution of SBS-PPA-modified binders. VA exhibited a smooth matrix, while the addition of 3% SBS resulted in dispersed polymeric domains forming a foam-like structure. The incorporation of

0.3% PPA refined this structure, reducing voids and enhancing polymer dispersion. At higher PPA dosages (0.6% and 0.9%), the binder developed a more compact and cross-linked network.

6. Based on the Overall Desirability (OD) analysis, the binder with 3% SBS and 0.3% PPA achieved the highest OD score of 0.539, reflecting the best balance of properties across all performance metrics, including penetration, softening point, ductility, rutting resistance, elastic recovery, and fatigue life. This formulation is recommended as the optimal modification level for SBS and PPA.

For the suggested optimum binder formation, further field studies are needed to evaluate long-term performance under real-world conditions to assess the practical effect of responding to traffic loads, environmental stresses, and aging.

Author Contributions: Conceptualization, A.H.A.; Methodology, M.J.A.-K. and A.M.M.; Formal analysis, A.H.A., M.J.A.-K., A.F.A.-a. and M.M.M.; Investigation, A.H.A. and Y.W.; Resources, A.H.A.; Data curation, A.F.A.-a. and M.M.M.; Writing—original draft, A.H.A., M.J.A.-K., A.F.A.-a., Y.W., A.M.M. and M.M.M.; Writing—review and editing, A.H.A., M.J.A.-K. and Y.W.; Visualization, A.M.M. All authors have read and agreed to the published version of the manuscript.

Funding: This research did not receive any specific grant from funding agencies in the public, commercial, or not-for-profit sectors.

Data Availability Statement: Data will be made available upon request to the corresponding author.

Conflicts of Interest: The authors declare that they have no known competing financial interests or personal relationships that could have appeared to influence the work reported in this paper.

References

1. Aljbouri, H.J.; Albayati, A.H. Effect of Nanomaterials on the Durability of Hot Mix Asphalt. *Transp. Eng.* **2023**, *11*, 100165. [CrossRef]
2. Al-Tameemi, A.F.; Wang, Y.; Albayati, A. Experimental Study of the Performance Related Properties of Asphalt Concrete Modified with Hydrated Lime. *J. Mater. Civ. Eng.* **2016**, *28*, 04015185. [CrossRef]
3. Wang, Y.; Latief, R.H.; Al-Mosawe, H.; Mohammad, H.K.; Albayati, A.; Haynes, J. Influence of Iron Filing Waste on the Performance of Warm Mix Asphalt. *Sustainability* **2021**, *13*, 13828. [CrossRef]
4. Baumgardner, G.; Hajj, E.Y.; Aschenbrener, T.B.; Hand, A.J. *Responsible Use of Polyphosphoric Acid (PPA) Modification of Asphalt Binders*; Technical report for the Federal Highway Administration: Washington, DC, USA, 2023.
5. Rossi, C.O.; Spadafora, A.; Teltayev, B.; Izmailova, G.; Amerbayev, Y.; Bortolotti, V. Polymer Modified Bitumen: Rheological Properties and Structural Characterization. *Colloids Surfaces A: Physicochem. Eng. Asp.* **2015**, *480*, 390–397. [CrossRef]
6. Gao, L.; Cai, N.; Fu, X.; He, R.; Zhang, H.; Zhou, J.; Kuang, D.; Liu, S. Influence of PPA on the Short-Term Antiaging Performance of Asphalt. *Adv. Civ. Eng.* **2021**, *2021*, 1–11. [CrossRef]
7. Cuciniello, G.; Leandri, P.; Filippi, S.; Presti, D.L.; Losa, M.; Airey, G. Effect of Ageing on the Morphology and Creep and Recovery of Polymer-Modified Bitumens. *Mater. Struct.* **2018**, *51*, 136. [CrossRef]
8. Alam, S.; Hossain, Z. Changes in Fractional Compositions of PPA and SBS Modified Asphalt Binders. *Constr. Build. Mater.* **2017**, *152*, 386–393. [CrossRef]
9. Yang, Z.; Zhang, X.; Yu, J.; Xu, W. Effects of Aging on the Multiscale Properties of SBS-Modified Asphalt. *Arab. J. Sci. Eng.* **2018**, *44*, 4349–4358. [CrossRef]
10. Ramayya, V.V.; Ram, V.V.; Krishnaiah, S.; Sandra, A.K. Performance of VG30 Paving Grade Bitumen Modified with Polyphosphoric Acid at Medium and High Temperature Regimes. *Constr. Build. Mater.* **2016**, *105*, 157–164. [CrossRef]
11. Liang, P.; Liang, M.; Fan, W.; Zhang, Y.; Qian, C.; Ren, S. Improving Thermo-Rheological Behavior and Compatibility of SBR Modified Asphalt by Addition of Polyphosphoric Acid (PPA). *Constr. Build. Mater.* **2017**, *139*, 183–192. [CrossRef]
12. Xiao, F.; Amirkhanian, S.; Wang, H.; Hao, P. Rheological Property Investigations for Polymer and Polyphosphoric Acid Modified Asphalt Binders at High Temperatures. *Constr. Build. Mater.* **2014**, *64*, 316–323. [CrossRef]
13. Jafari, M.; Babazadeh, A. Evaluation of Polyphosphoric Acid-Modified Binders Using Multiple Stress Creep and Recovery and Linear Amplitude Sweep Tests. *Road Mater. Pavement Des.* **2016**, *17*, 859–876. [CrossRef]
14. Cuadri, A.A.; Navarro, F.J.; Partal, P. Synergistic Ethylcellulose/Polyphosphoric Acid Modification of Bitumen for Paving Applications. *Mater. Struct.* **2020**, *53*, 1–13. [CrossRef]

15. Ma, F.; Li, C.; Fu, Z.; Huang, Y.; Dai, J.; Feng, Q. Evaluation of High Temperature Rheological Performance of Polyphosphoric Acid-SBS and Polyphosphoric Acid-Crumb Rubber Modified Asphalt. *Constr. Build. Mater.* **2021**, *306*, 124926. [CrossRef]
16. Li, C.; Li, Z.; Guo, T.; Chen, Y.; Liu, Q.; Wang, J.; Jin, L. Study on the Performance of SBS/Polyphosphoric Acid Composite Modified Asphalt. *Coatings* **2024**, *14*, 72. [CrossRef]
17. Wei, J.; Shi, S.; Zhou, Y.; Chen, Z.; Yu, F.; Peng, Z.; Duan, X. Research on Performance of SBS-PPA and SBR-PPA Compound Modified Asphalts. *Materials* **2022**, *15*, 2112. [CrossRef]
18. Pamplona, T.F.; Faxina, A.L. Effect of Polyphosphoric Acid on Asphalt Binders with Different Chemical Composition. In Proceedings of the 2015 Transportation Research Board 94th Annual Meeting, Washington, DC, USA, 11–15 January 2015.
19. Muslih, K.D.; Abbas, A.M. *Climate of Iraq, in The Geography of Iraq*; Springer International Publishing: New York, NY, USA, 2024; pp. 19–47.
20. Albayati, A.H. A Review of Rutting in Asphalt Concrete Pavement. *Open Eng.* **2023**, *13*, 20220463. [CrossRef]
21. *SCRB/R9*; General Specification for Roads and Bridges, S.R., Hot-Mix Asphalt Concrete Pavement. State Corporation of Roads and Bridges, Ministry of Housing and Construction: Baghdad, Republic of Iraq, 2003.
22. Baldino, N.; Marchesano, Y.; Mileti, O.; Lupi, F.; Gabriele, D. Thermo-Rheological Behaviour of Styrene-Butadiene-Styrene, Hard Plastics With or Without Graphene Oxide Modified Bitumens. *Case Stud. Constr. Mater.* **2024**, *20*, e03354. [CrossRef]
23. Dong, F.; Jiang, Y.; Yu, X.; Jin, Y.; Lu, J.; Wan, L.; Li, Z. Performance Restoration of Aged SBS-Modified Asphalt in RAP via Dry-Process SBS Modifier Diffusion at the Interface of Aggregate-Aged Asphalt-Virgin Asphalt. *Constr. Build. Mater.* **2024**, *453*, 139022. [CrossRef]
24. Badr, M.J.; Ismael, M.Q. Improvement Marshall Properties of Hot Mix Asphalt Concrete Using Polyphosphoric Acid. *J. Eng.* **2024**, *30*, 124–139. [CrossRef]
25. Johnson, C.; Bahia, H.; Wen, H. Practical Application of Viscoelastic Continuum Damage Theory to Asphalt Binder Fatigue Characterization. *Asph. Paving Technol.* **2009**, *75*, 597–638.
26. Hintz, C.; Velasquez, R.; Johnson, C.; Bahia, H. Modification and Validation of Linear Amplitude Sweep Test for Binder Fatigue Specification. *Transp. Res. Rec. J. Transp. Res. Board* **2011**, *2207*, 99–106. [CrossRef]
27. Niu, X.; Chen, Y.; Li, Z.; Guo, T.; Wang, J.; Jin, L. Study on the Performance and Modification Mechanism of Polyphosphoric Acid (PPA)/Styrene–Butadiene–Styrene (SBS) Composite Modified Asphalt. *Coatings* **2023**, *13*, 2003. [CrossRef]
28. Hossain, Z.; Braham, A.F.; Baumgardner, G. *Performance of Asphalts Modified with Polyphosphoric Acid*; TRC 1501 Final Report; National Academy of Sciences: Washington, DC, USA, 2017.
29. Saboo, N.; Kumar, R.; Kumar, P.; Gupta, A. Ranking the Rheological Response of SBS- and EVA-Modified Bitumen Using MSCR and LAS Tests. *J. Mater. Civ. Eng.* **2018**, *30*. [CrossRef]
30. Cao, Z.; Hao, Q.; Qu, X.; Qiu, K.; Zhao, R.; Liu, Q. Evolution of Structure and Properties of SBS-Modified Asphalt during Aging Process. *Buildings* **2024**, *14*, 291. [CrossRef]
31. Rani, S.R.; Ghabchi, M.R.; Zaman, M.; Andli, S.A. Rutting Performance of PPA-Modified Binders using Multiple Stress Creep and Recovery (MSCR) Test. In Proceedings of the IACMAG Symposium 2019, Gandhinagar, India, 5–7 March 2019.
32. Albayati, A.H.; Latief, R.H.; Al-Mosawe, H.; Wang, Y. Nano-Additives in Asphalt Binder: Bridging the Gap between Traditional Materials and Modern Requirements. *Appl. Sci.* **2024**, *14*, 3998. [CrossRef]

Disclaimer/Publisher's Note: The statements, opinions and data contained in all publications are solely those of the individual author(s) and contributor(s) and not of MDPI and/or the editor(s). MDPI and/or the editor(s) disclaim responsibility for any injury to people or property resulting from any ideas, methods, instructions or products referred to in the content.